Disaster risk, climate change, and poverty: assessing the global exposure of poor people to floods and droughts

Hessel C. Winsemius[1,3*], Brenden Jongman[2, 3], Ted I.E. Veldkamp[3], Stephane Hallegatte[2], Mook Bangalore[2,4], and Philip J. Ward[3]

[1] Deltares, Delft, [2] Global Facility for Disaster Reduction and Recovery, World Bank Group, Washington, DC, [3] Institute for Environmental Studies, Vrije Universiteit, Amsterdam, [4] Grantham Research Institute and Department of Geography and Environment, London School of Economics and Political Science, London

*Corresponding author. Email: hessel.winsemius@deltares.nl

ONLINE APPENDIX

Appendix A. Flood and drought modelling

A.1. Hydrological modelling

The basis of both the flood and drought indicators is the simulation of daily river discharge and runoff using a global hydrological model. For this project, we used simulations carried out using the global hydrological model PCR-GLOBWB (Van Beek and Bierkens, 2009; Van Beek *et al*., 2011). This model simulates daily discharge and runoff at a horizontal resolution of 0.5° x 0.5°.

The model was forced using daily meteorological fields of precipitation, temperature, and radiation for four different time-periods, namely: (a) 1960-1999, which represents the baseline climate; (b) 2010-2049 (representing 2030); (c) 2030-2069 (representing 2050); and (d) 2060-2099 (representing 2080). The meteorological data for the baseline climate are taken from the WATCH Forcing data (Weedon *et al*., 2011). The future meteorological data are provided by the ISI-MIP project, and consist of bias-corrected data (Hempel *et al*., 2013) for an ensemble of five Global Climate Models (GCMs) from the CMIP5 project (Taylor *et al*., 2012). The GCMs used are GFDL-ESM2M, HadGEM2-ES, IPSL-CM5A-LR, MIROC-ESM-CHEM, and NorESM1-M. For this study, we used climate projections based on two representative concentration pathways (RCPs), namely RCP 2.6 and RCP 8.5. The resolution of the input meteorological data sets for the current and future climate conditions is 0.5° x 0.5°.

For the simulations of floods and droughts, naturalized flow regimes were used, because the operation of reservoirs during flood and drought conditions is highly variable across the globe and requires detailed in-situ information about the flood and drought operation rules of each reservoir. The operations during floods and droughts may vary depending on many factors, for example: the (multi-purpose) use of the reservoir; the history of storage (e.g. after consecutive dry years, reservoir operators often maintain higher storage

levels); and the (non-)availability of forecast information or information on release strategies of upstream reservoirs. Therefore, reservoirs were included as if they were natural lakes.

A.2. Simulation of flood indicator

In this study, the indicator used to represent flooding is inundation depth greater than a given threshold (for example, inundation depths >0 m, >0.1 m, etc.). Here we selected a 0.1 m threshold, therefore including any flooded area of 0.1 meter and above. We used flood inundation maps at a horizontal resolution of 30" x 30" (ca. 1km x 1km at the equator). The maps are derived by downscaling of the results at lower resolution, applied on outputs of the hydrological model over current and future time-periods, using elevation data at much higher resolution (ca. 1km x 1 km) than the model resolution (ca. 50km x 50 km). These data are described in more detail in Winsemius *et al.* (2015). The method uses the GLOFRIS model cascade inundation downscaling technique, which is described in detail in Ward *et al.* (2013). Here, we provide a brief summary of this downscaling procedure.

Daily gridded flood volumes are simulated at a horizontal resolution of 0.5° x 0.5°, using the routing module of the PCR-GLOBWB model. From these daily flood volumes, annual time-series of gridded maximum flood volumes are extracted for the hydrological years 1960-1999. A Gumbel distribution is then fit through this time-series (excluding years with zero flood volume), and the resulting parameters of the Gumbel distribution are used to estimate flood volumes for different return periods, (where needed, conditional on the probability of exceedance of zero flood volume). This results in a set of maps showing the flood volume in m^3 of each 0.5° x 0.5° grid-cell for all return periods. These are then used as input in the GLOFRIS downscaling module, described in Winsemius *et al.* (2013) to derive maps showing inundation extent and depth at the high resolution of 30" x 30" (see for an example, figure 1 in the main text, top-left graph). Within the simulations, the assumption is

made that flood protection is absent. The granularity of the maps (horizontal resolution of 30" x 30") is good for representing wide floodplain areas (>1km in width), but may be too low to accurately represent all flood processes in riverine regions with steep topography. Here flood plains are usually quite narrow (i.e. < 1 km).

It should be noted that the inundation maps represent only riverine flooding, assuming the absence of flood protection measures. Moreover, they do not include coastal flooding, flooding from smaller streams, or flash floods.

A.3. Simulation of drought indicator

Hydrological drought conditions, or below-normal water availability, were identified using the widely-applied variable threshold level method (Hisdal and Tallaksen, 2003; Fleig *et al*., 2006). In this study we defined the monthly Q_{80}, the mean monthly streamflow that is exceeded 80 per cent of the time, as a measure for hydrological drought (Hisdal *et al*., 2001; Andreadis *et al*., 2005; Sheffield and Wood, 2007; Tallaksen *et al*., 2009; Corzo Perez *et al*., 2011; Van Loon and Van Lanen, 2012; Wada *et al*., 2013). Using monthly mean discharge values for the baseline scenario (EU-WATCH 1960-1999), simulated with PCR-GLOBWB (Van Beek *et al*., 2011), we calculated for each cell its monthly $Q_{80.}$ Following earlier studies (Lehner and Döll, 2001; Wada *et al*., 2013; Wanders and Wada, 2015), we determined the drought intensity for all combinations of GCM, RCP and time-period as the deficit volume below the Q_{80} threshold level as specified under the baseline scenarios (figure A1). Subsequently, monthly drought intensities per grid-cell were accumulated using the method developed by Lehner and Döll (2001) and Wanders and Wada (2015) whereby the accumulated volumes are set to zero each time the discharge is higher than the Q_{80} threshold level.

(a) Morocco **(b) Malawi**

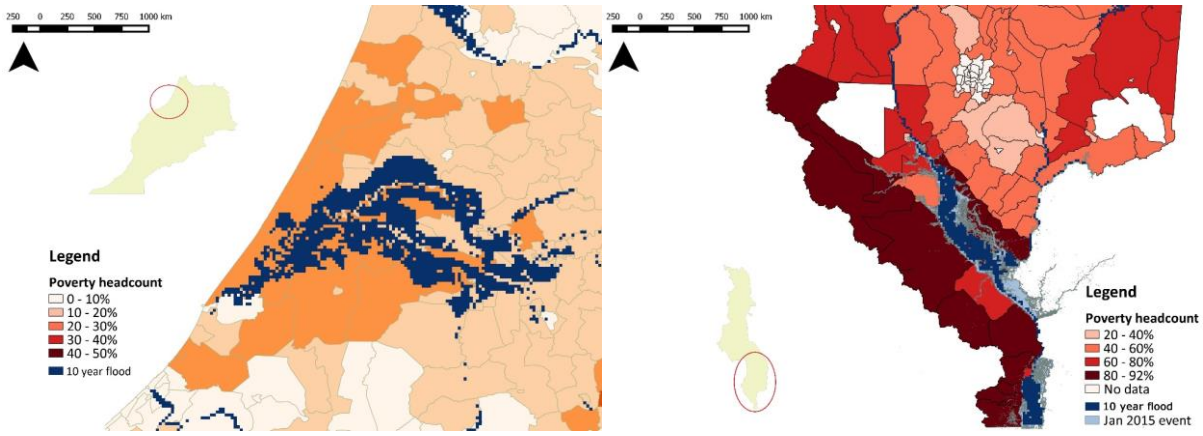

Figure A1. Overlay of poverty headcount maps at subnational level with a map showing 1 in 10 year flooding. Morocco is shown in left panel A. Source: Morocco High Commission for Planning (2013). Malawi is shown in right panel B. The 10 year flood refers to a 10-year return period flood. Sources: World Bank and Malawi Statistics Office (2013), UNOSAT (2015), German Space Agency (2015).

Using these values, we selected the maximum accumulated deficit volume for each hydrological year and a Gumbel distribution was fit through these time-series of maximum yearly standardized values (excluding the years with no deficits) (Engeland *et al.*, 2005; WMO, 2008). The parameters of the Gumbel distribution were used to estimate maximum yearly accumulated deficit volumes of each 0.5° x 0.5° grid-cell for different return periods, conditional on the probability of exceedance of zero discharge deficits. To enable comparison between rivers of different size, we standardized the maximum accumulated deficit volumes found per return period by dividing them by their long-term mean monthly discharge values.

$$V_{MAD\,i,y} = \max[\sum(0, \tau_{i,m} - Q_{i,m})]_y \quad \text{(A.1)}$$

$$S_{MAD\,i,RP} = \frac{V_{MAD\,i,RP}}{Q_{LTM,i}} \quad \text{(A.2)}$$

where V_{MAD} is the maximum accumulated deficit volume [m^3], i is the grid-cell considered, y and RP are the year or return period considered respectively, τ is the Q_{80} threshold [$m^3\ s^{-1}$], Q is the simulated monthly discharge [$m^3\ s^{-1}$] in month m, Q_{LTM} is the long-term mean

simulated monthly discharge, and S_{MAD} is the standardized maximum accumulated deficit volume (s).

The resulting maps express the relative intensity of drought conditions to long-term mean stream flow conditions and can be interpreted as the amount of time a long-term mean discharge would be needed to overcome the maximum accumulated deficit volume under a certain return period. In this study, we used the value of three months (of long-term mean discharge) as the indicator to represent droughts (for an example, see figure 1 of main text, bottom-left panel). The resolution of the maps represents drought conditions well for areas where droughts generally may be assumed to occur at a large scale (>50 km^2). In regions where drought conditions could be very localized, for example due to highly variable topography and high variability in water availability within a grid-cell, the results may be less representative.

A.4. Geographical uncertainty and sample size robustness

To guarantee anonymity of the interviewed households, the geographical locations of the clusters have been randomly allocated by DHS within a radius of maximum 2 km from the real location for urban areas, and 5 km for rural areas. We performed a sensitivity assessment by simulating 100 random replacements of all geographical locations with a radius of 2 km for urban and 5 km for rural areas, and computed the exposure for each of the 100 replacements. From the 100 results with random replacements, we assessed the uncertainty of the results due to uncertainty in geographical locations. We found no significant differences in results using the random location replacements and therefore we have not reported about this analysis in our results.

In addition, we assessed the uncertainty due to sample size by bootstrapping with 5,000 samples with replacement. In detail, per country, a sample was generated by drawing with

replacement, a set of households of equal size of the total amount of households in that country. We performed this for nationwide, urban and rural results respectively. If the expected value was positive ($I_p > 0$), we tested for a 95 per cent confidence for H($I_p > 0$). When the expected value was negative, we tested for a 95 per cent confidence for H($I_p < 0$).

A.5. Changes in risk under climate change

We assessed how climate change affects the poverty exposure bias, as well as the number of exposed people, by computing the poverty exposure bias as well as the annual average number of exposed people in 2030, 2050 and 2080, using the hazard maps representative for these periods and for 5 different GCMs.

We also computed the poverty exposure bias and annual exposed people using the hazard maps for the reference period (1960-1999) but established based upon the GCMs rather than the EU-WATCH reanalysis data set. Since the GCMs used contain bias due to unrepresented intra-annual and interannual variability (Johnson *et al*., 2011), we used the model-model difference in annual exposed people to establish changes in the exposure rather than the absolute outcomes.

Appendix B: Local scale poverty exposure analysis for floods

The national-scale analysis shows that some countries exhibit an over-exposure of poor people to floods and droughts, some show no difference, and others exhibit an over-exposure of non-poor people. This gives rise to the question of whether there is a similar variability in the exposure bias within regions of the countries. While the DHS data do not allow for analyses of the patterns within countries (as they are not representative at small scales), in this section we examine the exposure to floods using detailed poverty maps in two countries:

Malawi (Traditional Authority or TA-level, from World Bank and Malawi Statistics Office, 2013) and Morocco (commune-level, from Planning, 2013).

These poverty maps provide spatially explicit estimates of poverty, using income as a metric. In both Malawi and Morocco, poverty is defined as the percentage of people within a commune/district who earn less than US$1.25 per day in 2005 purchasing power parity (PPP) terms. This measure of poverty is distinctly different from the DHS wealth index. While the wealth index is a measure of assets and structural poverty (and is typically more long-lasting), the measure of poverty we use here is one of income or consumption (which is typically more variable). On the hazard side, we use the same data source for floods, selecting the 10-year return period flood.

We compare exposure to floods and poverty levels across 1689 communes (for Morocco) and across 370 TAs (for Malawi) for the whole country. This analysis yields similar results to the DHS analysis: for Morocco, we find a negative bias of -0.10 (-0.29 using DHS) and for Malawi a positive bias of 0.08 (0.18 using DHS).

However, there is clear evidence of overexposure of the poor in specific areas of the country, even though there is no bias at the national scale. Figure A1 shows an overlay of commune and district level poverty maps with modelled flood extents in parts of Morocco and Malawi. Specifically, North West Morocco, north of Kenitra, exhibits a high correlation of poverty and exposure; in Malawi, this is the case in the South, at the Shire Basin, close to the confluence with the Zambezi. As an example, in January 2015 the same area experienced a flood event which hit the poorest areas the hardest.

However, as described above, these national-level trends may hide significant heterogeneity within regions. Considering only the northwest of Morocco (left panel of figure A1), we now find a slightly PEB of 0.07 as opposed to the -0.24 that we found at the national level). For the south of Malawi (right panel of figure A1), we find a significantly large

exposure bias of 0.52 as opposed to 0.10 (not significant) at the national level. These findings support the hypothesis that we can find different biases occurring at different scales. Further, the identification of sub-national areas with a PEB may provide a rationale for targeting investments in these areas, concerning both protection ex-ante and disaster support ex-post.

These results suggest high variability of the PEB within countries. Differences exist between rural and urban areas, and across lower administrative units such as provinces and cities. While national level studies, such as our analysis with DHS surveys, are useful for starting the discussion on poverty impacts of natural hazards, local decision-makers may require the local level PEB to design their own poverty and risk management strategies. Ideally, such local analyses could make use of higher-resolution flood or drought maps and local household surveys designed to be representative at the local scale. For example, in Mumbai, local-scale flood data and household surveys revealed that an over-exposure of poor people to floods can be observed (Hallegatte *et al*., 2016), but varies at a very small scale, from one street to the next (Patankar, 2016).

One issue with DHS surveys – and almost all other household surveys – is that they have not been designed to be representative at small spatial scales. At best, they are representative at the spatial scale of a large province or area. Furthermore, the process used to select the surveyed households is not always reported explicitly, and often has to account for cost considerations that can bias the sample. We are well aware of this limit, and it implies that results should be interpreted with caution. The fact that we are working on a large sample of 52 countries compensates for the limit of the analysis at the country level.

Supplementary Figures

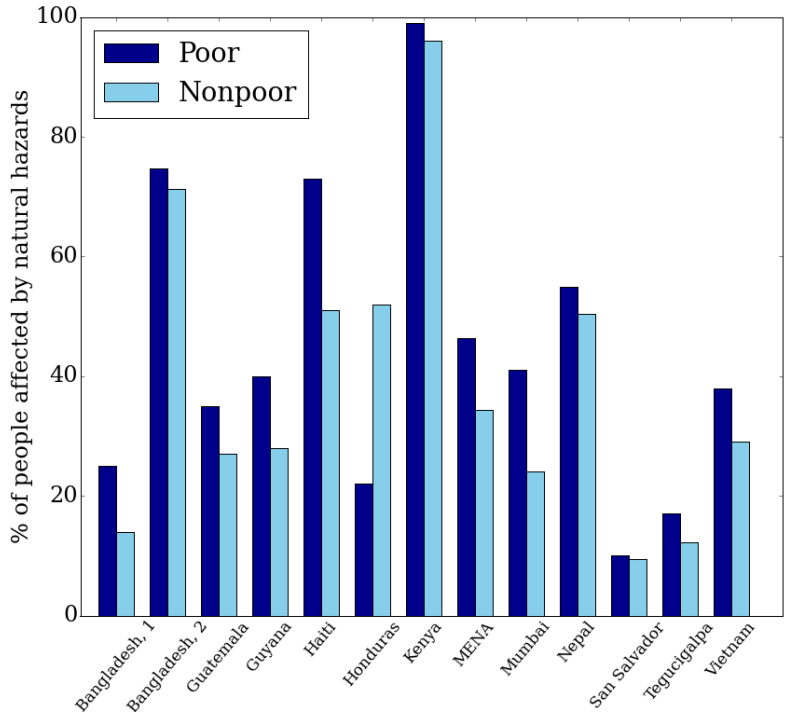

Figure A2. When a disaster hits, poor people are more likely to be affected.

Sources: Based on Akter and Mallick (2013) for Bangladesh (1) and del Ninno *et al.* (2001) for Bangladesh (2); Tesliuc and Lindert (2002) for Guatemala; Pelling (1997) for Guyana; Fuchs (2014) for Haiti; Carter *et al.* (2007) for Honduras; Opondo (2013) for Kenya; Wodon *et al.* (2014) for MENA; Baker *et al.* (2005) and Hallegatte *et al.* (2010) for Mumbai; Gentle *et al.* (2014) for Nepal; Fay (2005) for San Salvador and Tegucigalpa, and Nguyen (2011) for Vietnam.

Note: Based on thirteen case studies of past disasters, examining the exposure of poor and non-poor people through household surveys. Each study has a different definition of "poor" and "nonpoor" people. Exposure differs based on the type of hazard and context in which it occurs.

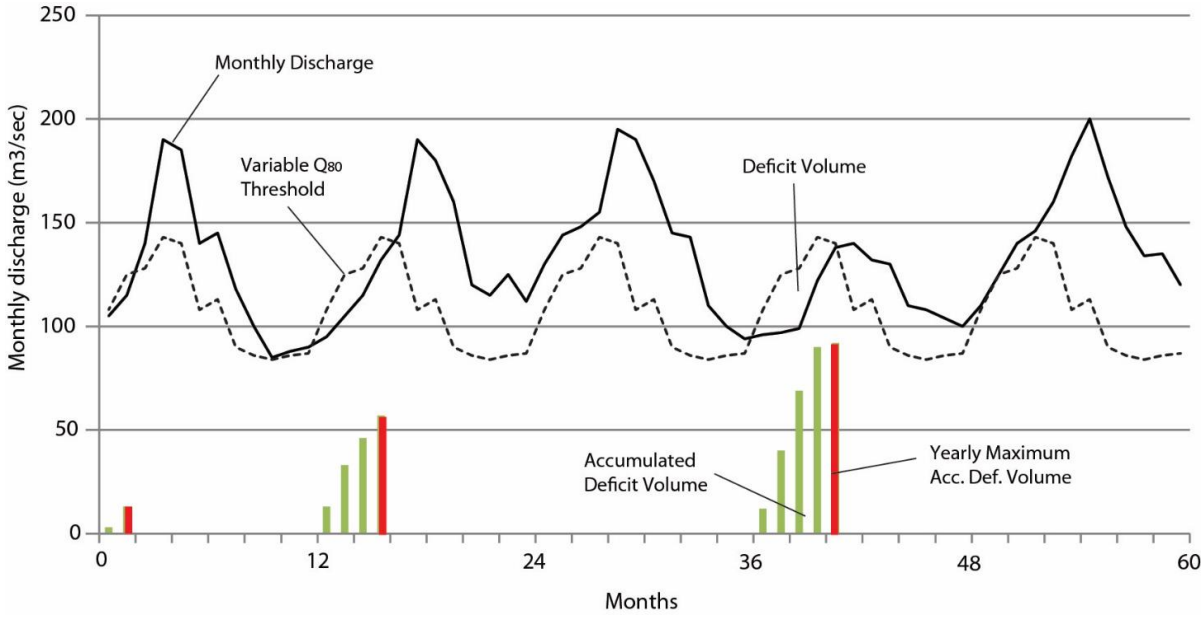

Figure A3. Definition of drought events and accumulated deficit volumes using a variable Q_{80} threshold level, i.e. varying heights of the threshold level throughout the year based on monthly Q_{80} values (after: Lehner and Döll, 2001).

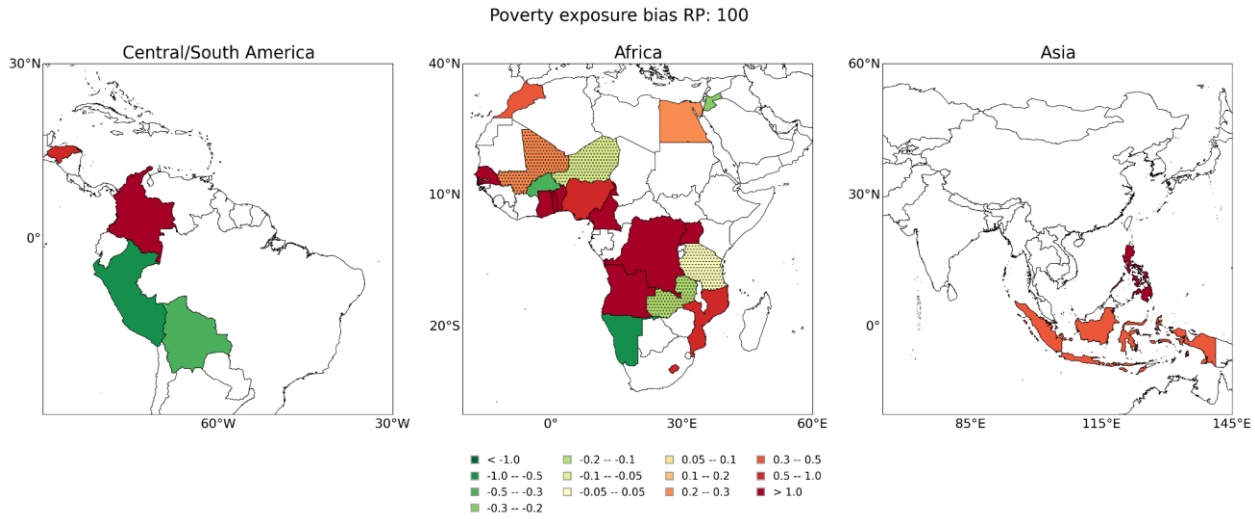

Figure A4. Same as figure 4 in the main text, but for urban households only. Note that the quintile subdivision used is based on urban households only.

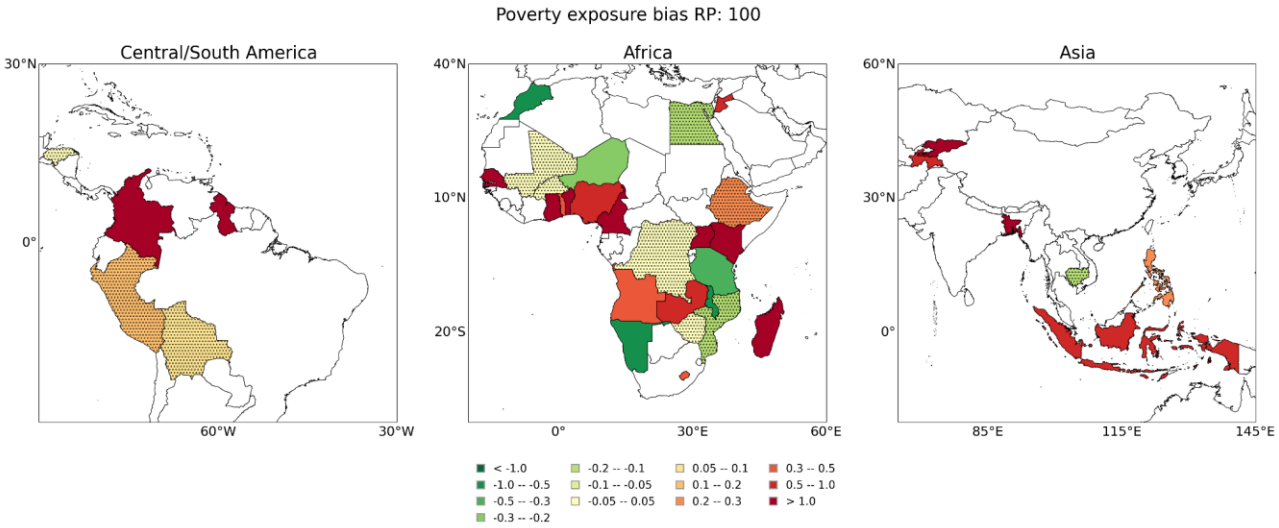

Figure A5. Same as figure 4 in the main text, but for rural households only. Note that the quintile subdivision used is based on rural households only.

References

Akter S and Mallick B (2013) The poverty–vulnerability–resilience nexus: evidence from Bangladesh. *Ecological Economics* **96**, 114-124.

Andreadis KM, Clark EA, Wood AW, Hamlet AF and Lettenmaier DP (2005) Twentieth-century drought in the conterminous United States. *Journal of Hydrometeorology* **6**(6), 985-1001.

Baker J, Basu R, Cropper M, Lall S and Takeuchi A (2005) Urban poverty and transport: the case of Mumbai, World Bank Policy Research Working Paper 3693.

Carter MR, Little PD, Mogues T and Negatu W (2007) Poverty traps and natural disasters in Ethiopia and Honduras. *World Development* **35**(5), 835-856.

Corzo Perez GA, van Huijgevoort MHJ, Voß F and van Lanen HAJ (2011) On the spatio-temporal analysis of hydrological droughts from global hydrological models. *Hydrology and Earth System Sciences* **15**(9), 2963-2978.

del Ninno C, Dorosh PA, Smith LC and Roy D (2001) The 1998 floods in Bangladesh: disaster impacts, household coping strategies, and response, International Food Policy Research Institute.

Engeland K, Hisdal H and Frigessi A (2005) Practical extreme value modelling of hydrological floods and droughts: a case study. *Extremes* **7**(1), 5-30.

Fay M (ed)], Ruggeri Laderchi, C, Wellenstein A, Moser C, Winton A, Moser A, Monkkomen P, Woolcock M, Cohan L and McEvoy Karla (2005) *The Urban Poor in Latin America*, Directions in Development, Washington, DC: World Bank.

Fleig AK, Tallaksen LM, Hisdal H and Demuth S (2006) A global evaluation of streamflow drought characteristics. *Hydrology and Earth System Sciences* **10**(4), 535-552.

Fuchs A (2014) Shocks and poverty in Haiti, Presentation at the conference "Poverty and Climate Change Flagship - An Overview of the LAC Region", World Bank, Washington, DC, September 4, 2104.

Gentle P, Thwaites R, Race D and Alexander K (2014) Differential impacts of climate change on communities in the middle hills region of Nepal. *Natural Hazards* **74**(2), 815-836.

German Space Agency (2015) January 2015 flood extent of Malawi Event, [Available at] http://www.masdap.mw/layers/geonode:flood_terrasarx_bydlr.

Hallegatte S, Bangalore M, Bonzanigo L, Fay M, Kane T, Narloch U, Rozenberg J, Treguer D and Vogt-Schilb A (2016) *Shock Waves: Managing the Impacts of Climate Change on Poverty*, World Bank Publications, Washington DC, [Available at] https://openknowledge.worldbank.org/handle/10986/22787.

Hallegatte S, Ranger N, Bhattacharya S, Bachu M, Priya S, Dhore K, Rafique F, Mathur P, Naville N, Henriet F, Patwardhan A, Narayanan K, Ghosh S, Karmakar S, Patnaik U, Abhayankar A, Pohit S, Corfee-Morlot J and Herweijer C (2010), Flood risks, climate change impacts and adaptation benefits in Mumbai: an initial assessment of socio-economic consequences of present and climate change induced flood risks and of possible adaptation options, OECD Environment Working Papers, No. 27, OECD Publishing, Paris.

Hempel S, Frieler K, Warszawski L, Schewe J and Piontek F (2013) A trend-preserving bias correction – the ISI-MIP approach. *Earth System Dynamics* **4**(2), 219-236.

Hisdal H, Stahl K, Tallaksen LM and Demuth S (2001) Have streamflow droughts in Europe become more severe or frequent? *International Journal of Climatology* **21**(3), 317-333.

Hisdal H and Tallaksen LM (2003) Estimation of regional meteorological and hydrological drought characteristics: a case study for Denmark. *Journal of Hydrology* **281**(3), 230-247.

Johnson F, Westra S, Sharma A and Pitman AJ (2011) An assessment of GCM skill in simulating persistence across multiple time scales. *Journal of Climate* **24**(14), 3609-3623.

Lehner B and Döll P (2001) Europe's droughts today and in the future, in B. Lehner, T. Henrichs, P. Döll and J. Alcamo (eds), *EuroWasser – Model-based Assessment of European Water Resources and Hydrology in the Face Of Global Change*, World Water Series No. 5, Center for Environmental Systems Research, University of Kassel, Kassel, Germany.

Morocco High Commission for Planning (2013) Poverty, vulnerability, and inequality indicators, [Available at] http://www.hcp.ma/Pauvrete-vulnerabilite-et-inegalite_r99.html.

Nguyen VK (2011) Building Livelihood Resilience in Changing Climate.

Opondo DO (2013) Erosive coping after the 2011 floods in Kenya. *International Journal of Global Warming* **5**(4), 452-466.

Patankar A (2016) The exposure, vulnerability and ability to adapt of poor households to recurrent floods in Mumbai, in *Shock Waves: Managing the Impacts of Climate Change on Poverty*, Climate Development Series, Washington, DC: World Bank.

Pelling M (1997) What determines vulnerability to floods; a case study in Georgetown, Guyana. *Environment and Urbanization* **9**(1), 203-226.

Sheffield J and Wood EF (2007) Characteristics of global and regional drought, 1950–2000: analysis of soil moisture data from off-line simulation of the terrestrial hydrologic

cycle. *Journal of Geophysical Research* **112**(D17), D17115, doi:10.1029/2006JD008288.

Tallaksen LM, Hisdal H and van Lanen, HAJ (2009) Space–time modelling of catchment scale drought characteristics. *Journal of Hydrology* **375**(3–4), 363-372.

Taylor KE, Stouffer RJ and Meehl GA (2012) An overview of CMIP5 and the experiment design. *Bulletin of the American Meteorological Society* **93**(4), 48-498.

Tesliuc E and Lindert K (2002) Vulnerability: a quantitative and qualitative assessment, Guatemala Poverty Assessment Program, World Bank, Washington, DC [Available at] http://web.worldbank.org/archive/website00955A/WEB/PDF/GUAPA_VU.PDF.

UNOSAT (2015) January 2015 flood extent of Malawi Event, [online] Available from: http://www.masdap.mw/.

Van Beek LPH and Bierkens MFP (2009) The global hydrological model PCR-GLOBWB: conceptualization, parameterization and verification, Utrecht, [Available at] http://vanbeek.geo.uu.nl/suppinfo/vanbeekbierkens2009.pdf.

Van Beek LPH, Wada Y and Bierkens MFP (2011) Global monthly water stress: 1. Water balance and water availability. *Water Resources Research* **47**(7), W07517.

Van Loon, AF and Van Lanen HAJ (2012) A process-based typology of hydrological drought. *Hydrology and Earth System Sciences* **16**(7), 1915-1946.

Wada Y, van Beek LPH, Wanders N and Bierkens MFP (2013) Human water consumption intensifies hydrological drought worldwide. *Environmental Research Letters* **8**(3), 1-14.

Wanders N and Wada Y (2015) Human and climate impacts on the 21st century hydrological drought. *Journal of Hydrology* **526**, 208-220.

Ward PJ, Jongman B, Weiland FS, Bouwman A, van Beek R, Bierkens MFP, Ligtvoet W and Winsemius HC (2013) Assessing flood risk at the global scale model setup, results, and sensitivity. *Environmental Research Letters* **8**, 044019.

Weedon GP, Gomes S, Viterbo P, Shuttleworth WJ, Blyth E, Österle H, Adam JC, Bellouin N, Boucher O and Best M (2011) Creation of the WATCH Forcing Data and its use to assess global and regional reference crop evaporation over land during the twentieth century. *Journal of Hydrometeorology* **12**(5), 823-848.

Winsemius HC, Aerts JCJH, van Beek LPH, Bierkens MFP, Bouwman A, Jongman B, Kwadijk JCJ, Ligtvoet W, Lucas PL, van Vuuren DP and Ward PJ (2015) Global drivers of future river flood risk. *Nature Climate Change* **6**(4), 381-385.

Winsemius HC, Van Beek LPH, Jongman B, Ward PJ and Bouwman A (2013) A framework for global river flood risk assessments. *Hydrology and Earth System Sciences* **17**(5), 1871-1892.

WMO (World Meteorological Organization) (2008) Manual on Low-flow Estimation and Prediction, Operational Hydrology Report No. 50.

Wodon Q, Liverani A, Joseph G and Bougnoux N (eds) (2014) *Climate Change and Migration: Evidence from the Middle East and North Africa*, World Bank Studies, Washington, DC.

World Bank and Malawi Statistics Office (2013) Malawi Poverty Map.